

# Oscillating instanton solutions in curved space

Bum – Hoon Lee<sup>†§1</sup> Chul H. Lee<sup>¶2</sup> Wonwoo Lee<sup>§3</sup> Changheon Oh<sup>¶4</sup>

<sup>¶</sup>*Department of Physics, Hanyang University, Seoul 133-791, Korea*

<sup>†</sup>*Department of Physics and BK21 Division, Sogang University, Seoul 121-742, Korea*

<sup>§</sup>*Center for Quantum Spacetime, Sogang University, Seoul 121-742, Korea*

## Abstract

We investigate oscillating instanton solutions of a self-gravitating scalar field between degenerate vacua. We show that there exist  $O(4)$ -symmetric oscillating solutions not only in de Sitter but also in both flat and anti-de Sitter space. The geometry of these solutions is finite and preserves the  $Z_2$  symmetry. The nontrivial solution corresponding to tunneling is possible only if the effect of gravity is taken into account. We present numerical solutions of these instantons including the phase diagram of solutions and the variation of energy densities. Furthermore, we construct the phase space of all our solutions in terms of the parameters of the present work. Our solutions can be interpreted as solutions describing an instanton-induced domain wall or braneworld-like object rather than a kink-induced domain wall or braneworld. The oscillating instanton solutions have a thick wall and the solutions can be interpreted as a mechanism providing nucleation of the thick wall for topological inflation.

PACS numbers: 04.62.+v, 98.80.Cq

---

<sup>1</sup>*email:bhl@sogang.ac.kr*

<sup>2</sup>*email:chulhoon@hanyang.ac.kr*

<sup>3</sup>*email:warrior@sogang.ac.kr*

<sup>4</sup>*email:och0423@hanyang.ac.kr*

# 1 Introduction

The interpolating solution between degenerate vacua in curved space can be the solution representing formation of a domain wall or a braneworld-like object with  $Z_2$  symmetry if the thin-wall approximation scheme is used in the theory. Moreover, the solution after the analytic continuation expands, from an observer's point of view on the wall, without eating up bulk(inside and outside) spacetime. Can the braneworld or domain wall have nontrivial internal structure? The structure can be made with oscillating instanton solutions. What is the meaning of this internal structure? Can the number of oscillations indicate certain criteria based on specific parameters? In order to get the answers to the above questions, we need to obtain oscillating solutions, interpret the meaning of the solutions, and construct a phase space of all allowed oscillating solutions.

In the absence of gravity, instantons are usually defined as solutions with a finite action to the classical field equations in Euclidean space obeying appropriate boundary conditions. The Yang-Mills instantons are also finite action solutions and have been studied extensively in gauge theories [1, 2] as well as in string theory [3, 4], and references therein. In gravitational theory, there are several kinds of instantons [5]. Instantons should also be solutions to the Euclidean Einstein equations. Some instantons usually cannot be analytically continued to Lorentzian. Others can be analytically continued to Lorentzian. Instantons may be related to the semiclassical description of quantum gravity. However, this issue is beyond the scope of the present work and is therefore not being discussed here.

In this work, we consider tunneling phenomena in a double-well potential. Classically, a particle trapped in one well cannot penetrate through the potential barrier of that well, thus unaffected by the presence of the other well. However, if the central potential barrier is not infinitely high, there is tunneling between the two minima. The tunneling process is quantum mechanically described by the Euclidean solution obeying appropriate boundary conditions. The Euclidean solution interpolates between two different classical vacua. There exist two kinds of Euclidean solutions describing tunneling phenomena in the double-well potential. One, which is for tunneling in an asymmetric double-well potential, corresponds to a bounce solution. The bounce solution describes the decay of a background vacuum state. The other, which is for tunneling in a symmetric double-well potential, corresponds to an instanton solution. The instanton solution, in this case, describes a general shift in the ground state energy of the classical vacuum due to the presence of an additional potential well, lifting the classical degeneracy [6].

The instanton solution in one dimension is equivalent to a static soliton in  $(1+1)$  dimensions. Thus, the method for kink solution in two dimensions can be employed for studying the instanton solution in one dimension. The Euclidean equation of motion can be treated like a one-particle equation of motion with an evolution parameter playing the role of time in the inverted potential. A particle starts at the top of one hill at minus infinity in Euclidean time and arrives at the top of the other hill at plus infinity. The Euclidean action for the tunneling solution can be calculated easily using the fact that the Euclidean energy of an instanton is

equal to zero in the system. This action is identical to the energy of a static solution of the  $(1+1)$ -dimensional soliton theory. In addition, the action has the same value as the action obtained in connection with the WKB approximation of the splitting in energies of the two lowest levels for the symmetric double-well potential. In semiclassical approximation, the action is dominated by classical configuration in evaluating the path integral. For field theoretical solutions with  $O(4)$  symmetry, the Euclidean equation of motion has an additional term, which can be interpreted as a damping term. Thus, it is difficult to obtain the  $O(4)$ -symmetric instanton solution in this system when gravity is switched off. The damping term can be changed into the anti-damping term not only in de Sitter (dS) space but also in both flat and anti-de Sitter (AdS) space when gravity is taken into account [7].

The bounce solution is related to the nucleation of a true (false) vacuum bubble describing decay of a background vacuum state. The process has been studied within various contexts for several decades. It was first investigated in Ref. [8] and developed in both flat [9] and curved spacetime [10, 11]. A homogeneous Euclidean configuration in which the scalar field fluctuates simultaneously at the top of the potential barrier was investigated in Ref. [12] and further studied in Ref. [13]. As a special case of the true vacuum bubble, a vacuum bubble with a finite-sized background after nucleation was studied in Ref. [14]. The decay of false monopoles with a gauge group was also studied using the thin-wall approximation [15]. The bubble or brane resulting from flux tunneling was studied in a 6-dimensional Einstein-Maxwell theory [16].

The mechanism for nucleation of a false vacuum bubble in a true vacuum background has also been studied within various contexts. Nucleation of a large false vacuum bubble in dS space was obtained in Ref. [17] and nucleation with a global monopole in Ref. [18]. The mechanism for nucleation of a small false vacuum bubble was obtained in the Einstein gravity with a nonminimally coupled scalar field [19], with Gauss-Bonnet term in Ref. [20], and using Brans-Dicke type theory [21]. The classification of vacuum bubbles including false vacuum bubbles in the dS background in the Einstein gravity was obtained in Ref. [22], in which the transition rate and the size of the instanton solution were evaluated in the space, as the limiting case of large true vacuum bubble or large false vacuum bubble.

The oscillating solution with  $O(4)$  symmetry in dS space was first studied in Ref. [23], where the authors found the solution to oscillating scalar field  $\Phi$  in fixed background. They adopted the fact that the role of damping term in the particle analogy picture can be changed into that of anti-damping term in dS space if the evolution parameter exceeds half of a given range. The oscillation means that the field in their solutions oscillates back and forth between the two sides of the potential barrier. The analytic computation as the solution of a self-gravitating scalar field and meanings of this solution were further studied in Ref. [22]. We have observed that the interpolating solutions are possible even in AdS space if the local maximum value of the potential is positive. The solutions have exact  $Z_2$  symmetry and give rise to geometry of a finite size. We employed a homogeneous and static scalar field which has a constant value of  $\Phi$  everywhere in Euclidean space [7]. Thus, it is impossible that the solution has an infinite size because of the infinite cost of energy.

In the absence of gravity, the spectrum of small perturbations about the bounce solution has exactly one negative mode [24]. When gravity is taken into account, the problem becomes more complex [25]. On the other hand, the spectrum about the instanton solution between degenerate vacua has no negative mode. Thus we expect that the spectrum about our solutions will not have any negative modes.

The paper is organized as follows: in the next section we set up the basic framework for this work. We consider the tunneling process for the symmetric double-well potential and study the boundary conditions for our present work in detail. The boundary conditions analyzed in this work can be applicable to other cases including bounce solutions. In Sec. III, we present numerical oscillating instanton solutions in curved space. We consider the tunneling process not only in dS space but also in both flat and AdS space when the local maximum value of the potential is positive. We also examine the variation in the thickness of the wall and the energy density as the number of oscillations increased. Additionally, we examine numerically which solutions among oscillating solutions are relatively probable. In Sec. IV, we analyze the properties of oscillating instanton solutions and construct the phase space of all our solutions in terms of the two parameters for this work. The phase space of solutions exhibits the behaviors that occur when the number of oscillations increases and indicates the regions where there are no solutions depending on the parameters. In Sec. V, we summarize and discuss our results. We interpret the physical meaning of our oscillating solutions with thick walls.

## 2 Setup and boundary conditions

The vacuum-to-vacuum transition amplitude called the generating functional for Green's function can serve as a starting point for the non-perturbative treatment of the theory. In the path integral formalism, it can be visualized as the summation over all possible paths moving from the initial state to the final state. The transition amplitude in semiclassical approximation is dominated by those paths for which the Euclidean action difference is stationary. Thus, the tunneling amplitude can be evaluated in terms of the classical configuration and be represented as  $Ae^{-\Delta S}$  in this approximation, where the leading semiclassical exponent  $\Delta S$  is the difference between the Euclidean action corresponding to a classical solution and the background action itself. The pre-factor  $A$  is from the first order quantum correction [6, 24].

Let us consider the following action:

$$S = \int_{\mathcal{M}} \sqrt{-g} d^4x \left[ \frac{R}{2\kappa} - \frac{1}{2} \nabla^\alpha \Phi \nabla_\alpha \Phi - U(\Phi) \right] + \oint_{\partial\mathcal{M}} \sqrt{-h} d^3x \frac{K - K_o}{\kappa}, \quad (1)$$

where  $g \equiv \det g_{\mu\nu}$ ,  $\kappa \equiv 8\pi G$ ,  $R$  denotes the curvature scalar of spacetime  $\mathcal{M}$ ,  $K$  and  $K_o$  are traces of the extrinsic curvatures of  $\partial\mathcal{M}$  in the metric  $g_{\mu\nu}$  and  $\eta_{\mu\nu}$ , respectively, and the second term on the right-hand side is the boundary term [26]. The gravitational field equations can be obtained properly from a variational principle with this boundary term. This term is also necessary to obtain the correct action.

We reconsider the tunneling process for the symmetric double-well potential in curved space as in our previous work [7]. The potential  $U(\Phi)$ , which represents the energy density of a homogeneous and static scalar field, has two degenerate minima

$$U(\Phi) = \frac{\lambda}{8} \left( \Phi^2 - \frac{\mu^2}{\lambda} \right)^2 + U_0. \quad (2)$$

The cosmological constant is given as  $\Lambda = \kappa U_0$ , hence the space will be dS, flat, or AdS depending on whether  $U_0 > 0$ ,  $U_0 = 0$ , or  $U_0 < 0$ . We will make an attempt to obtain oscillating instanton solutions describing tunneling between degenerate vacua in these backgrounds.

To evaluate  $\Delta S$  and show the existence of the solution, one has to take the analytic continuation to Euclidean. We assume the  $O(4)$  symmetry for both the geometry and the scalar field as in Ref. [10]

$$ds^2 = d\eta^2 + \rho^2(\eta) [d\chi^2 + \sin^2 \chi (d\theta^2 + \sin^2 \theta d\phi^2)]. \quad (3)$$

In this case  $\Phi$  and  $\rho$  depend only on  $\eta$ , and the Euclidean field equations for them can be written in the form:

$$\Phi'' + \frac{3\rho'}{\rho} \Phi' = \frac{dU}{d\Phi} \quad \text{and} \quad \rho'' = -\frac{\kappa}{3} \rho (\Phi'^2 + U), \quad (4)$$

respectively and the Hamiltonian constraint is given as

$$\rho'^2 - 1 - \frac{\kappa\rho^2}{3} \left( \frac{1}{2} \Phi'^2 - U \right) = 0. \quad (5)$$

To maintain the solution the constraint requires a delicate balance among the terms. Otherwise the solution can cause qualitatively incorrect behavior [27].

Now we have to consider the boundary conditions to solve Eqs. (4) and (5). There are two kinds of method. One is an initial value problem, in which we impose initial conditions for the equations. For this work, initial conditions are the values of the fields  $\rho$  and  $\Phi$  or their derivatives  $\rho'$  and  $\Phi'$  at  $\eta = 0$  as follows:

$$\rho|_{\eta=0} = 0, \quad \frac{d\rho}{d\eta}\Big|_{\eta=0} = 1, \quad \Phi|_{\eta=0} = \Phi_o, \quad \text{and} \quad \frac{d\Phi}{d\eta}\Big|_{\eta=0} = 0, \quad (6)$$

where the first condition means that the space including a solution is a geodesically complete space. The second condition is from Eq. (5). The fourth condition  $\Phi' = 0$  is from the regularity condition as can be seen the first equation in Eq. (4). However, the third condition for the initial value of  $\Phi$  is not determined. One should find the initial value of  $\Phi$  using the undershoot-overshoot procedure. This procedure is made for the non-oscillating bounce solution, i.e. a one-crossing solution as we will explain about that in the next section. Some initial  $\Phi_o$  will give the overshooting, in which the value of  $\Phi$  at late  $\eta$  will go beyond  $\mu/\sqrt{\lambda}$ . Some other initial value of  $\Phi_o$  will give the undershoot, in which the value of  $\Phi$  at late  $\eta$  does not reach at  $\mu/\sqrt{\lambda}$ . Thus, the value  $\Phi_o$  must be an intermediate position between undershoot and overshoot [9]. The existence of oscillating solutions are secreted within the undershoot as we will see in the

next section. The other is a boundary value problem or a two boundary value problem. We impose conditions specified at  $\eta = 0$  and  $\eta = \eta_{max}$ . For this work, we choose the values of the field  $\rho$  and derivatives of the field  $\Phi$  as follows:

$$\rho|_{\eta=0} = 0, \quad \rho|_{\eta=\eta_{max}} = 0, \quad \frac{d\Phi}{d\eta}\Big|_{\eta=0} = 0, \quad \text{and} \quad \frac{d\Phi}{d\eta}\Big|_{\eta=\eta_{max}} = 0. \quad (7)$$

The  $\eta_{max}$  is the maximum value of  $\eta$  and will have a finite value. The conditions are useful for solutions with  $Z_2$  symmetry.

In order to solve the Euclidean field Eqs. (4) and (5) numerically, we first rewrite equations in terms of dimensionless variables as in Ref [19]:

$$\frac{\lambda U(\Phi)}{\mu^4} = \tilde{U}(\tilde{\Phi}), \quad \frac{\lambda \Phi^2}{\mu^2} = \tilde{\Phi}^2, \quad \mu\eta = \tilde{\eta}, \quad \mu\rho = \tilde{\rho}, \quad \text{and} \quad \frac{\mu^2}{\lambda}\kappa = \tilde{\kappa}. \quad (8)$$

These variables give

$$\tilde{U}(\tilde{\Phi}) = \frac{1}{8} \left( \tilde{\Phi}^2 - 1 \right)^2 + \tilde{U}_0, \quad (9)$$

and the Euclidean field equations for  $\Phi$  and  $\rho$  are

$$\tilde{\Phi}'' + \frac{3\tilde{\rho}'}{\tilde{\rho}}\tilde{\Phi}' = \frac{d\tilde{U}}{d\tilde{\Phi}} \quad \text{and} \quad \tilde{\rho}'' = -\frac{\tilde{\kappa}}{3}\tilde{\rho}(\tilde{\Phi}'^2 + \tilde{U}), \quad (10)$$

respectively. The Hamiltonian constraint is given as

$$\tilde{\rho}'' - 1 - \frac{\tilde{\kappa}\tilde{\rho}^2}{3} \left( \frac{1}{2}\tilde{\Phi}'^2 - \tilde{U} \right) = 0. \quad (11)$$

We now make comments on boundary conditions more precisely to solve Eqs. (10) and (11) numerically. As we already mentioned the boundary conditions, there are two kinds of condition. The relaxation method is one of methods to solve a two boundary value problem. However we do not know the exact value of  $\tilde{\eta}_{max}$  in our case, thus we can not impose the boundary condition at  $\tilde{\eta} = \tilde{\eta}_{max}$ . In this work we employ shooting method using the adaptive step size Runge-Kutta as an initial value problem in Ref. [28]. For this procedure we choose the initial values of  $\tilde{\Phi}(\tilde{\eta}_{initial})$ ,  $\tilde{\Phi}'(\tilde{\eta}_{initial})$ ,  $\tilde{\rho}(\tilde{\eta}_{initial})$ , and  $\tilde{\rho}'(\tilde{\eta}_{initial})$  at  $\tilde{\eta} = \tilde{\eta}_{initial}$  as follows:

$$\begin{aligned} \tilde{\Phi}(\tilde{\eta}_{initial}) &\sim \tilde{\Phi}_0 + \frac{\epsilon^2}{16}\tilde{\Phi}_0 \left( \tilde{\Phi}_0^2 - 1 \right) + \frac{\epsilon^3}{48} \left( 3\tilde{\Phi}_0^2 - 1 \right), \\ \tilde{\Phi}'(\tilde{\eta}_{initial}) &\sim \frac{\epsilon}{8}\tilde{\Phi}_0 \left( \tilde{\Phi}_0^2 - 1 \right) + \frac{\epsilon^2}{16} \left( 3\tilde{\Phi}_0^2 - 1 \right), \\ \tilde{\rho}(\tilde{\eta}_{initial}) &\sim \epsilon, \\ \tilde{\rho}'(\tilde{\eta}_{initial}) &\sim 1, \end{aligned} \quad (12)$$

where  $\tilde{\eta}_{initial} = 0 + \epsilon$  and  $\epsilon \ll 1$ . If we find the initial value  $\tilde{\Phi}_0$ , other conditions are given by Eqs. (12). Furthermore we impose additional conditions implicitly. To avoid a singular solution

at  $\tilde{\eta} = \tilde{\eta}_{max}$  in Eq. (10) and demand the  $Z_2$  symmetry, the conditions  $d\tilde{\Phi}/d\tilde{\eta} \rightarrow 0$  and  $\tilde{\rho} \rightarrow 0$  as  $\tilde{\eta} \rightarrow \tilde{\eta}_{max}$  are needed. In this work we require that a value of  $d\tilde{\Phi}/d\tilde{\eta}$  goes to the value smaller than  $10^{-6}$  as  $\tilde{\eta} \rightarrow \tilde{\eta}_{max}$ , because the exact value of  $\tilde{\eta}_{max}$  is not known.

We will examine the energy density of the oscillating region of a solution to observe a domain wall structure. The action of the one-dimensional instanton has the form

$$s_o = \int_{-\infty}^{\infty} \left[ \frac{1}{2} \Phi'^2 + U \right] d\tau = \frac{2\mu^3}{3\lambda},$$

where we take the potential as in Eq. (2). To obtain a solution with finite action, it is required that  $\Phi' \rightarrow 0$  and  $U \rightarrow 0$  as  $\tau \rightarrow \pm\infty$ . This action is equal to the surface tension or the surface energy density of the wall [9]. When gravity is taken into account, the situation is more complicated. To simplify matters, we only consider the Euclidean action of the bulk part in Eq. (1)

$$S_E = \int_{\mathcal{M}} \sqrt{g_E} d^4x_E \left[ -\frac{R_E}{2\kappa} + \frac{1}{2} \Phi'^2 + U \right] = 2\pi^2 \int \rho^3 d\eta [-U], \quad (13)$$

where  $R_E = 6[1/\rho^2 - \rho'^2/\rho^2 - \rho''/\rho]$  and we used Eqs. (4) and (5). Thus the contributions from the geometry and kinetic energy in Euclidean are added to be the potential effectively. On the other hand, the action in Ref. [10] is rewritten as

$$S_E = -\frac{12\pi^2}{\kappa} \int \rho d\eta \left( 1 - \frac{\kappa\rho^2 U}{3} \right), \quad (14)$$

where the authors used integration by parts. Because they were only interested in the action difference between two solutions that agree at infinite, the surface term from integration by parts was regarded as harmless. The minus sign appeared in the action is related to the fact that the Euclidean action for Einstein gravity is not positive-definite, which is known as the conformal factor problem in Euclidean quantum gravity [29]. However, this issue is not central to the problem and therefore we will not discuss the issue any more in the present paper. In this work, we will examine the relative probability among the solutions. We employ Eq. (13) for the present work. The volume energy density in this work has the form

$$\xi \equiv -\mathcal{H} = - \left[ -\frac{R}{2\kappa} + \frac{1}{2} \Phi'^2 + U \right] = U. \quad (15)$$

We will check the change of the density with respect to the evolution parameter  $\eta$  in the next section.

### 3 Oscillating instanton solutions between degenerate vacua

In Ref. [23], the authors found oscillating solutions between the dS-dS vacuum states. They had shown that there exist two kinds of oscillating solutions, one is the case with an asymmetric

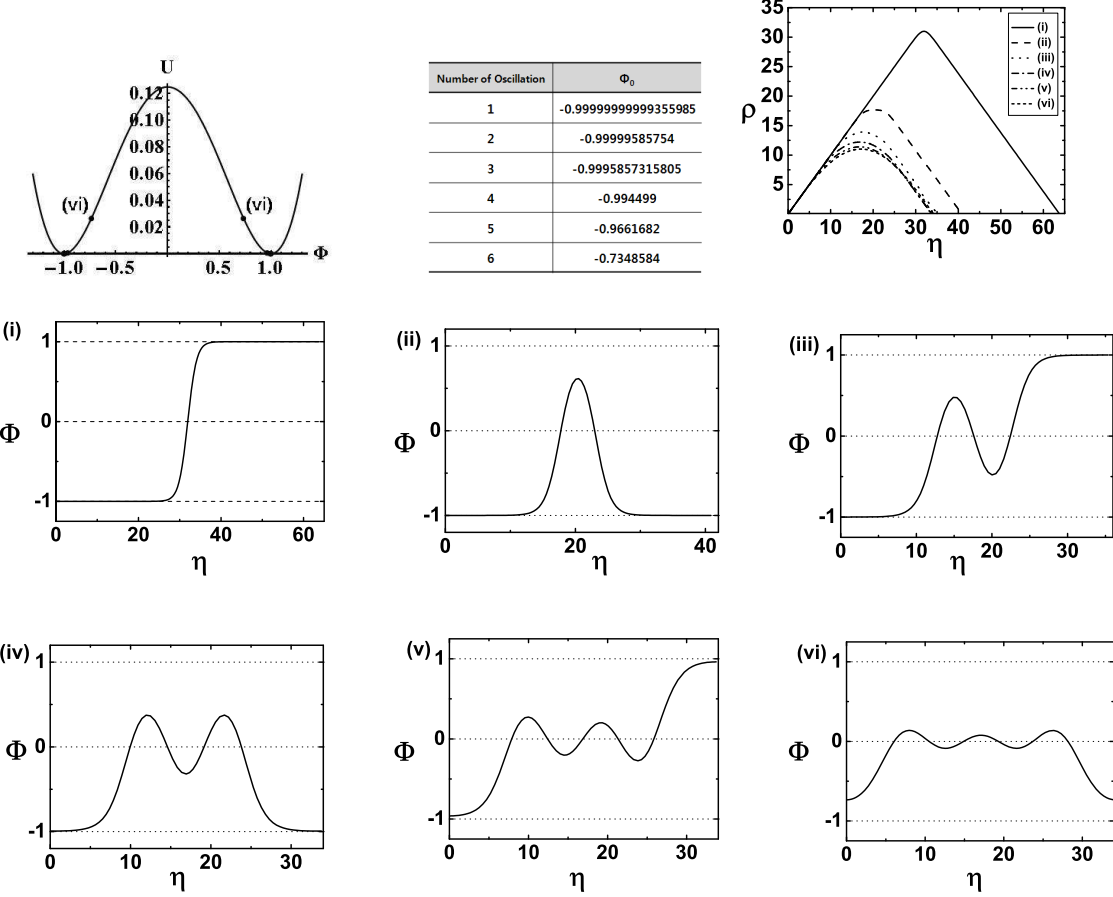


Figure 1: The numerical solutions represent oscillating instanton solutions between flat-flat degenerate vacua.

double-well potential and the other the case with a symmetric potential. They showed how the maximum allowed number  $n_{max}$  depends on the parameters of the theory, in which  $n$  denotes the crossing number of the potential barrier by oscillating solutions. However, they did rather than solving coupled equations simultaneously, the fixed dS background was employed for  $\rho$ . This is a good approximation for  $U_o \gg 0$  [23]. We will solve the equations simultaneously, because we are interested in the situation not only in dS but also in both flat and AdS background. The one-crossing solution,  $n = 1$ , corresponds to the instanton solutions [7]. The two-crossing solution,  $n = 2$ , was considered as the type of the double-bounce solution or anti-double-bounce solution [30], in which the authors interpreted the double-bounce solution as the spontaneous pair-creation of true vacuum bubbles separated by a wall. Additionally, we examine the variation of the energy density to see the structure of the domain wall and the oscillating behavior depending on  $\tilde{\kappa}$  and  $\tilde{\kappa}\tilde{U}_o$ .

Figure 1 shows oscillating instanton solutions representing tunneling starting from left vac-

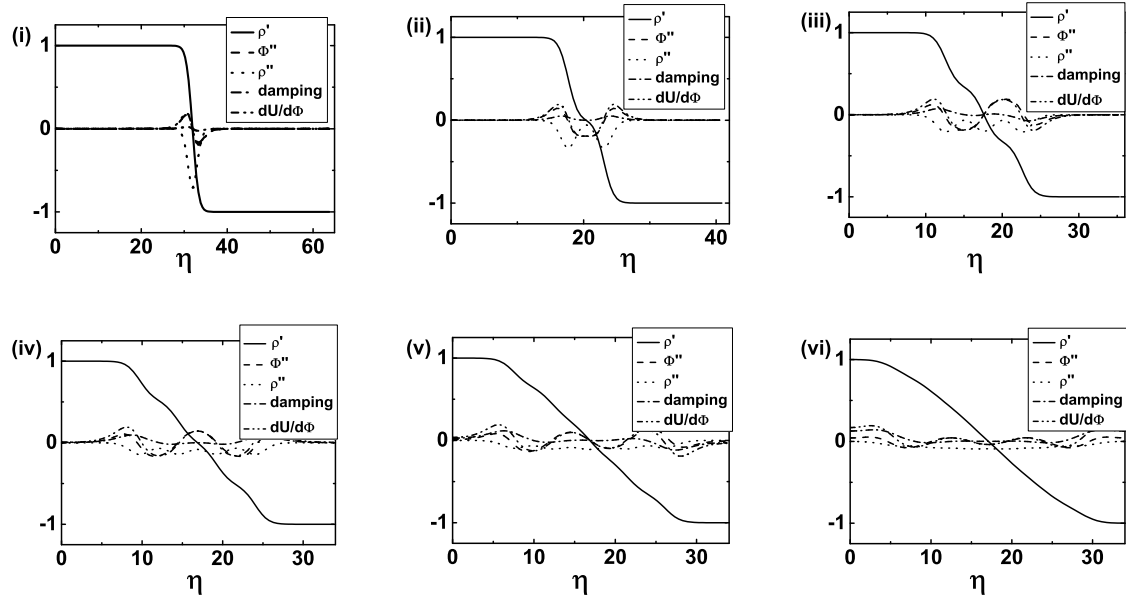


Figure 2: Variation of terms in equations of motion between flat-flat degenerate vacua.

uum state in the case of flat-flat degenerate vacua. We take  $\tilde{\kappa} = 0.2$  for all cases. The first figure illustrates the potential, in which the number  $n$  denotes the number of the crossing. The maximum number  $n_{max} = 6$ . The second figure illustrates the initial point  $\tilde{\Phi}_o$  for each number of oscillations. As expected, the number of oscillations increases as the initial point,  $\tilde{\Phi}(\tilde{\eta}_{initial}) = \tilde{\Phi}_o$ , moves away from the vacuum state. The third figure illustrates the solutions of  $\tilde{\rho}$ . We can see that the size of the geometry with a solution decreases as the number of crossing increases because the period of the evolution parameter  $\tilde{\eta}_{max}$  decreases as the starting point moves away from the vacuum state. The solution of  $\tilde{\rho}$  is  $\tilde{\eta}$  in fixed flat space. Thus, the straight evolution line of  $\tilde{\rho}$  near the vacuum state indicate flat space. The figure (i) illustrates the one-crossing solution,  $n = 1$ , of the field  $\tilde{\Phi}$ . The figure (ii) illustrates the two-crossing solution,  $n = 2$ . There does not exist this type of the solution including bounce solutions when gravity is switched off. However, the solution is somewhat different from the double-bounce solution in Ref. [30]. Since our solution of  $\tilde{\Phi}$  does not asymptotically approach the other vacuum state, it is difficult that we interpret our solution as the double-instanton solution or the spontaneous pair-creation of instanton solutions. The figure (iii)-(vi) illustrate the  $n$ -crossing solution,  $n = 3, 4, 5, 6$ . The figures (i), (iii), and (v) illustrate the tunneling starting from the left vacuum state to the right vacuum state. The figures (ii), (iv), and (vi) illustrate solutions going back to the starting point after oscillations. This type of solutions is possible only if gravity is taken into account. The maximum number of oscillations is determined by the parameters  $\tilde{\kappa}$  and  $\tilde{U}_o$  observed in Ref. [23].

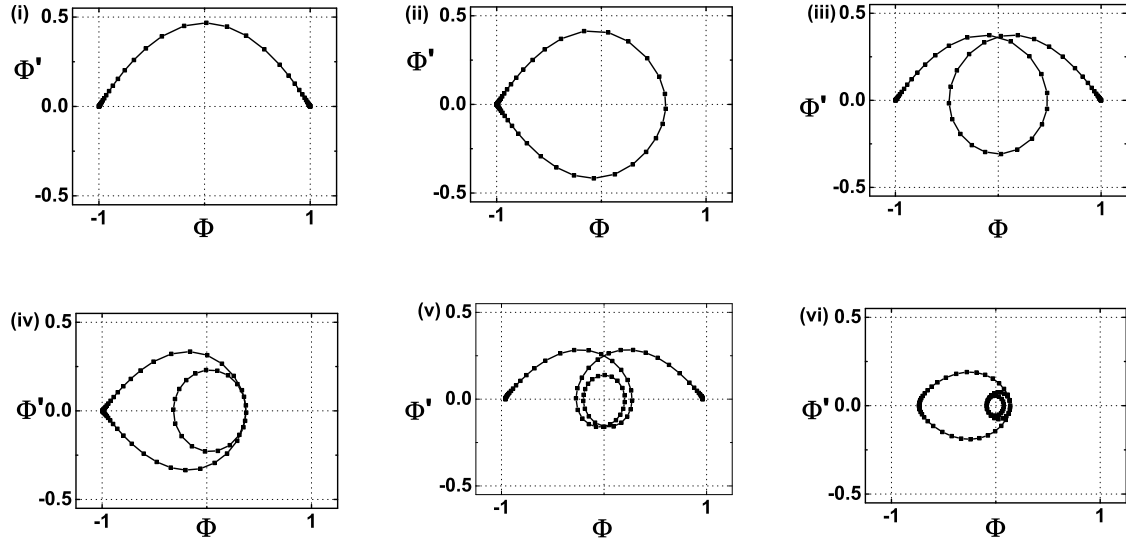


Figure 3: The behavior of the solutions in the  $\Phi$ - $\Phi'$  plane using the phase diagram method. The case is belong to the tunneling between flat-flat degenerate vacua.

Figure 2 shows the variation of terms,  $\tilde{\rho}'$ ,  $\tilde{\Phi}'$ ,  $\tilde{\rho}''$ ,  $\frac{3\tilde{\rho}'}{\tilde{\rho}}\tilde{\Phi}'$ , and  $d\tilde{U}/d\tilde{\Phi}$ , with respect to  $\tilde{\eta}$  in Eqs. (10) and (11). In figures (i) - (vi), we see that the sign change of  $\tilde{\rho}'$  from positive to negative occurs at the half period due to the  $Z_2$  symmetry. The value of  $\tilde{\rho}'$  at near initial and final value of  $\tilde{\eta}$  means the flat space at that point. The value of  $\tilde{\rho}'$  spans from 1 to  $-1$  in all figures. The transition region of  $\tilde{\rho}'$  means the rolling duration in the inverted potential. In that region, every other terms also have dynamical behavior. The value of  $\tilde{\Phi}''$  representing an acceleration of the particle in the inverted potential increases, decreases, and is zero at the half period. The graph is odd function. The value of  $\tilde{\rho}''$  has always a negative value or zero as an even function according to Eq. (10). The damping term also increases, decreases, and is zero as an odd function. The term  $d\tilde{U}/d\tilde{\Phi}$  has the same property. The figures (i), (iii), and (v) representing tunneling show that  $\tilde{\rho}'$ ,  $\tilde{\Phi}''$ , damping, and  $d\tilde{U}/d\tilde{\Phi}$  change the sign simultaneously at the half period. The figures (ii), (iv), and (vi) representing solutions going back to the starting point show that only  $\tilde{\rho}'$  change the sign at the half period. All of behaviors represented in each figure can be understood with  $Z_2$  symmetry.

The behavior of the solutions in the  $\tilde{\Phi}(\tilde{\eta})$ - $\tilde{\Phi}'(\tilde{\eta})$  plane using the phase diagram method is shown in Fig. 3. The figure (i) illustrates the phase diagram of a one-crossing solution, in which the trajectory is restricted to the upper half region in the diagram. It is the turning point from the damping phase to the anti-damping phase when  $\tilde{\Phi}'$  is the maximum value and  $\tilde{\Phi}$  is the first zero. The value of  $\tilde{\Phi}$  spans from  $-1$  to  $+1$  and  $\tilde{\Phi}'$  from zero via maximum value, about 0.49, to zero with symmetry about the  $y$ -axis. The figure (ii) illustrates the diagram of a two-crossing solution, in which the trajectory does not reach the opposite point  $\tilde{\Phi} = 1$  and does return the

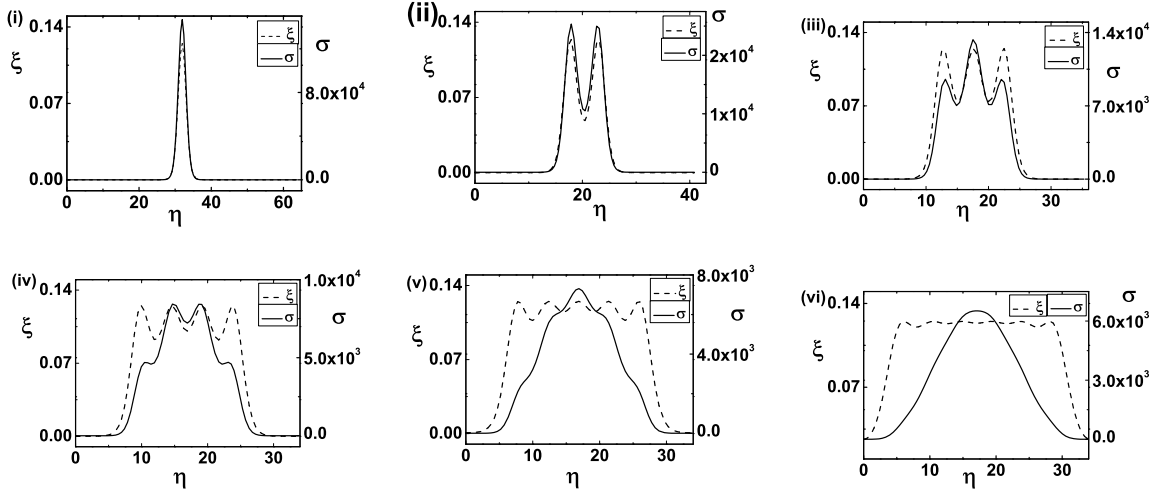


Figure 4: The diagram of energy density of each solutions. In each figure, the solid line denotes the surface energy density  $\sigma$  and the dotted line denotes the volume energy density  $\xi$ .

starting point  $\tilde{\Phi} = -1$ . When the trajectory goes back,  $\tilde{\Phi}'$  is negative with symmetry about the  $x$ -axis. It is the turning point from the damping phase to the anti-damping phase when  $\tilde{\Phi}'$  is the second zero and  $\tilde{\Phi}$  is positive. The figure (iii) illustrates the diagram of three-crossing solution. It is the turning point when  $\tilde{\Phi}'$  is the negative maximum value and  $\tilde{\Phi}$  is the second zero. The figure (iv) illustrates the diagram of four-crossing solution. It is the turning point when  $\tilde{\Phi}'$  is the third zero and  $\tilde{\Phi}$  is negative. The figure (v) illustrates the diagram of five-crossing solution. It is the turning point when  $\tilde{\Phi}'$  is positive and  $\tilde{\Phi}$  is the second zero. The figure (vi) illustrates the diagram of six-crossing solution. It is the turning point when  $\tilde{\Phi}'$  is the third zero and  $\tilde{\Phi}$  is positive. The figures (i), (iii), and (v) have symmetry about the  $y$ -axis. The figures (ii), (iv), and (vi) have symmetry about the  $x$ -axis. The maximum value of  $\tilde{\Phi}'$  decreases as the number of crossing increases.

Figure 4 shows the diagram of the energy density of each solutions. In each figure, the solid line denotes the surface energy density  $\sigma$  and the dotted line denotes the volume energy density  $\xi$  in Eq. (15). The surface energy density means the value after the integration of variables except for  $\eta$ . The peaks represent the rolling phase in the valley of the inverted potential. The maximum value  $\xi_{max}$  is equivalent to  $U_{top}$ . The number of peaks is equal to the number of crossing. The peaks broaden in range near  $U_{top}$  as the number of crossing increases. The surface energy density has also peaks. However, the shape of the peaks becomes smooth and broadens as the number of crossing increases. As can be seen from the figure (vi), the thickness of the wall increases as the number of oscillations increases.

We now consider oscillating instanton solutions between dS-dS degenerate vacua with  $\tilde{U}_o > 0$ . The numerical solutions in this case are shown in Fig. 5, in which we take  $\tilde{U}_o = 0.5$  and  $\tilde{\kappa} = 0.04$  for all figures. The figure (i) illustrates the solution of  $\tilde{\Phi}$  for a one-crossing solution

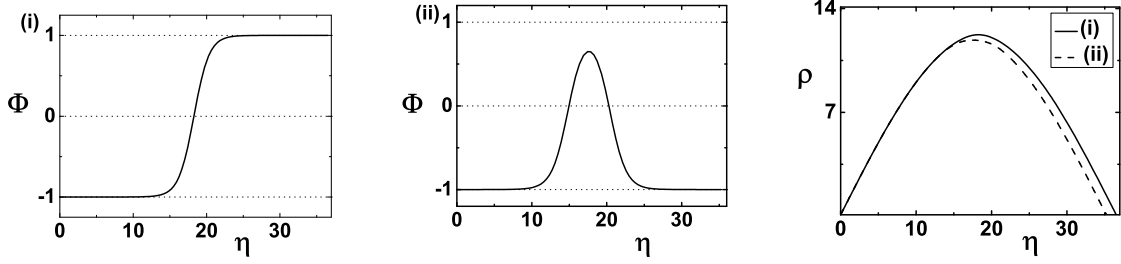


Figure 5: The numerical solutions between dS-dS degenerate vacua.

and the figure (ii) for a two-crossing solution. The figure (iii) illustrates the solution of each  $\tilde{\rho}$ . The solution of  $\tilde{\rho}$  is  $\sqrt{\frac{3}{\tilde{\kappa}U_o}} \sin \sqrt{\frac{\tilde{\kappa}U_o}{3}}\eta$  in fixed dS space. Thus, the graph of sine function type near vacuum states indicates dS space.

Figure 6 shows the collections of variation of terms in equations of motion, phase diagrams, and the diagram of energy density between dS-dS degenerate vacuum states. The figure (i) correspond to a one-crossing solution and the figure (ii)s correspond to a two-crossing solution. In the second figure, the maximum value of  $\tilde{\Phi}'$  is about 0.47. In third and sixth figures, the mountain-shaped graph of the surface energy density is owing to the integration of variables in de Sitter space. The volume energy density and the surface energy density are always positive. The initial and final region of  $\tilde{\rho}'$  in first and fourth figures exhibit cosine function type because the solution near vacuum states indicates dS space.

Next, let us consider oscillating instanton solutions between AdS-AdS degenerate vacua with  $\tilde{U}_o < 0$ . The numerical solutions in this case are shown in Fig. 7, in which we take  $\tilde{U}_o = -0.02$  and  $\tilde{\kappa} = 0.4$  for all figures. The third figure illustrates the solution of each  $\tilde{\rho}$ . The solution of  $\tilde{\rho}$  is  $\sqrt{\frac{3}{\tilde{\kappa}|\tilde{U}_o|}} \sinh \sqrt{\frac{\tilde{\kappa}|\tilde{U}_o|}{3}}\eta$  in fixed AdS space. Thus, the graph of hyperbolic sine function type near vacuum states indicates AdS space.

Figure 8 shows the collections of variation of terms in equations of motion, phase diagrams, and the diagram of energy density between AdS-AdS degenerate vacuum states. The figure (i)s correspond to a one-crossing solution and the figure (ii)s correspond to a two-crossing solution. In third and sixth figures, the dented region between peaks of the surface energy density is owing to the integration of variables in anti-de Sitter space. The volume energy density and the surface energy density are negative in AdS region and become positive in the valley of the inverted potential, i.e. the dS region. The initial and final region of  $\tilde{\rho}'$  in first and fourth figures exhibit the hyperbolic cosine function type because the solution near vacuum states indicates AdS space.

Let us now examine which solutions among oscillating solutions are relatively probable. Instead of subtracting the background action from the instanton action, we compare the action of

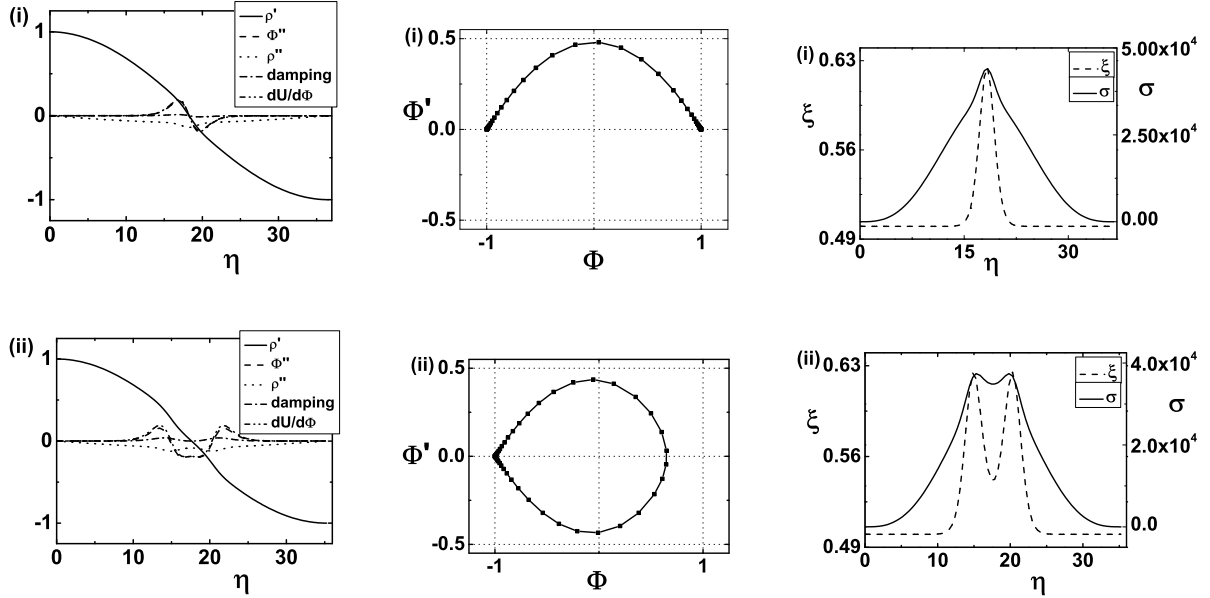


Figure 6: Variation of terms in equations of motion, phase diagrams, and the diagram of energy density between dS-dS degenerate vacua.

oscillating solutions with the action of the one-crossing instanton. Table 1 shows each action of solutions. We obtained the numerical action of oscillating solutions from data. In the integration, we employ an additional normalization process because we use dimensionless quantities for our numerical calculation. Thus we have normalized  $\Delta \tilde{S}_n$  as the difference between the action of the  $n$ -crossing solution and that of the one-crossing solution divided by a  $|\tilde{S}_1|$  as follows:

$$\Delta \tilde{S}_n \equiv \frac{\Delta \tilde{S}_n}{|\tilde{S}_1|} = \frac{\tilde{S}_n - \tilde{S}_1}{|\tilde{S}_1|} \quad (16)$$

where  $\tilde{S}_n$  denotes the action of the  $n$ -crossing solution. Our results are in Table 1, in which  $(\tilde{\kappa}, \tilde{U}_o)$  is  $(0.04, 0.5)$ ,  $(0.2, 0)$ , and  $(0.4, -0.02)$  respectively. Our results show that, as predicted, the transition amplitude is suppressed by an increase in oscillation number.

## 4 Properties of oscillating instanton solutions between degenerate vacua

In previous section, we obtained various properties of oscillating solutions between dS-dS, flat-flat, and AdS-AdS degenerate vacua. We make an attempt to obtain that the phase space of

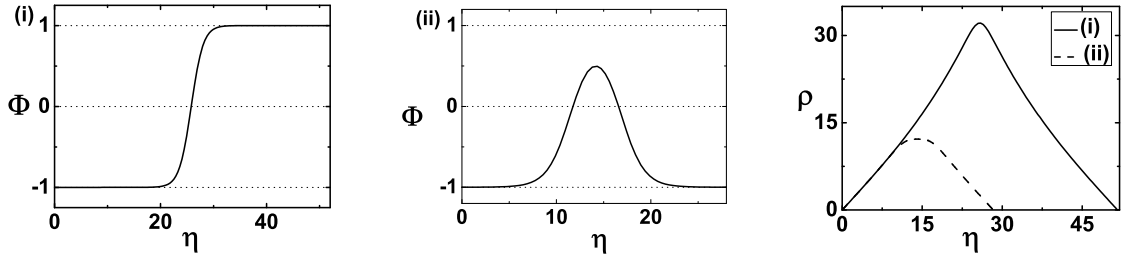


Figure 7: The numerical solutions between AdS-AdS degenerate vacua.

Table 1:  $\Delta S_n$  of Oscillating solutions between dS-dS, flat-flat, and AdS-AdS degenerate vacua.

Oscillation number	dS-dS case( $\Delta \tilde{S}_n$ )( $e^{-\Delta \tilde{S}_n}$ )	flat-flat( $\Delta \tilde{S}_n$ )( $e^{-\Delta \tilde{S}_n}$ )	AdS-AdS( $\Delta \tilde{S}_n$ )( $e^{-\Delta \tilde{S}_n}$ )
1	-544000(0)(1)	-403752(0)(1)	-152000(0)(1)
2	-511000(0.061)(0.941)	-161000(0.601)(0.548)	-39300(0.903)(0.405)
3	-490000(0.099)(0.906)	-114726(0.716)(0.489)	-30234(0.925)(0.396)
4	-479000(0.119)(0.887)	-101000(0.750)(0.472)	-28384(0.930)(0.395)
5	-475000(0.127)(0.881)	-96000(0.762)(0.467)	-
6	-473000(0.131)(0.878)	-94700(0.765)(0.465)	-

solutions in terms of the parameters  $\tilde{\kappa}$  and  $\tilde{\kappa}\tilde{U}_o$ . The parameter  $\tilde{\kappa}$  is the ratio between the gravitational constant, or Planck mass, and the mass scale in the theory,  $\tilde{\kappa} = \frac{\mu^2}{\lambda}\kappa = \frac{8\pi\mu^2}{M_p^2\lambda}$ , whereas the parameter  $\tilde{\kappa}\tilde{U}_o$  is related to the cosmological constant as  $\Lambda/\mu^2$ . Many questions arise in this stage. The first one is how many oscillating solutions are allowed in given  $\tilde{\kappa}$  and  $\tilde{U}_o$ . The second one is whether the number of oscillations depends on these parameters. What is the whole phase space of solutions according to parameter regions if the number depends on the parameters? The third one is what the different behaviors of solutions is among dS-dS, flat-flat, and AdS-AdS. To answer to these questions, we try to make the phase space of solutions in terms of  $\tilde{\kappa}$  and  $\tilde{\kappa}\tilde{U}_o$ . For  $\tilde{\kappa} \ll 1$ , the effect of gravity is negligible. However, when  $\tilde{\kappa}$  approaches to order one, the effect of gravity is important. To make the phase space of solutions, we collect data on  $\tilde{U}_o$ , which makes the difference of the maximum number of oscillations,  $n_{max}$ , for a given  $\tilde{\kappa}$ . We then obtain a specific  $\tilde{U}_o$  which determines the minimum number of oscillations,  $n_{min}$ . Finally, we employ the method of least squares [28] to obtain the relationship between

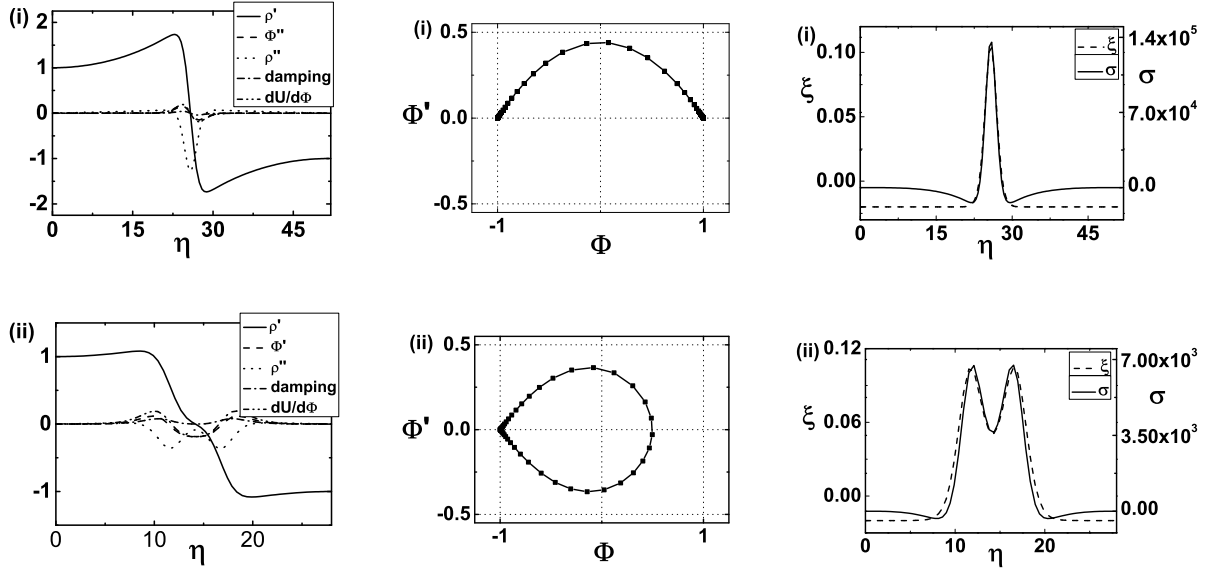


Figure 8: Variation of terms in equations of motion, phase diagrams, and the diagram of energy density between AdS-AdS degenerate vacua.

two parameters in given data sets of  $\tilde{\kappa}$  and  $\tilde{\kappa}\tilde{U}_o$ . Oscillating numbers appeared to be linearly related to the parameters.

Figure 9 shows the behaviors of oscillating solutions in terms of  $\tilde{\kappa}$  and  $\tilde{\kappa}\tilde{U}_o$ . The value of  $\tilde{\kappa}$  is limited to  $0 \leq \tilde{\kappa} \leq 1$ . At the point  $\tilde{\kappa} = 0$ , or  $M_p = \infty$ , gravity is switched off. The  $y$ -axis represents no gravity. We expect that there is no solution with  $O(4)$  symmetry when gravity is switched off. In each figure, we use the notation  $(n_{min}, n_{max})$ , where  $n_{min}$  means the minimum number of oscillations and  $n_{max}$  the maximum number of oscillation in given parameters. For example,  $(n_{min}, n_{max}) = (1, 1)$  means that the minimum number of oscillation is 1 and the maximum number of oscillation 1. The figures (i) and (ii) illustrate the number of oscillations in the case of dS-dS degenerate vacua. In fig. (i), there is the zone representing no solution in the right upper region. When the parameter  $\tilde{\kappa}$  or  $\tilde{U}_o$  increased, the evolution period of  $\tilde{\eta}_{max}$  diminished in general. The  $\tilde{\rho}$  approaches at  $\tilde{\rho}_{max}$  before the field arrive at the other vacuum state in the inverted potential. Thus, there is no solution because of the short evolution period. In other words, the instanton solution can not fit inside the Euclideanized dS background in the strong gravity limit. When the parameter  $\tilde{\kappa}$  or  $\tilde{U}_o$  decreased, the evolution period of  $\tilde{\eta}_{max}$  and the maximum number of oscillations increased. The figure (ii) illustrates the zone with the small value of parameters in fig. (i). The upper zone allows  $n_{min} = 1$ , whereas the lower zone allows  $n_{min} = 2$  divided by the solid line. The figure (iii) illustrates the behaviors of the oscillating solutions in the case of AdS-AdS degenerate vacua. In this case,  $(n_{min}, n_{max}) = (1, 1)$  is not allowed. If there is a tunneling solution, then there are oscillating solutions together. This is a different properties from the dS-dS case. In addition, there is a no-solution parameter

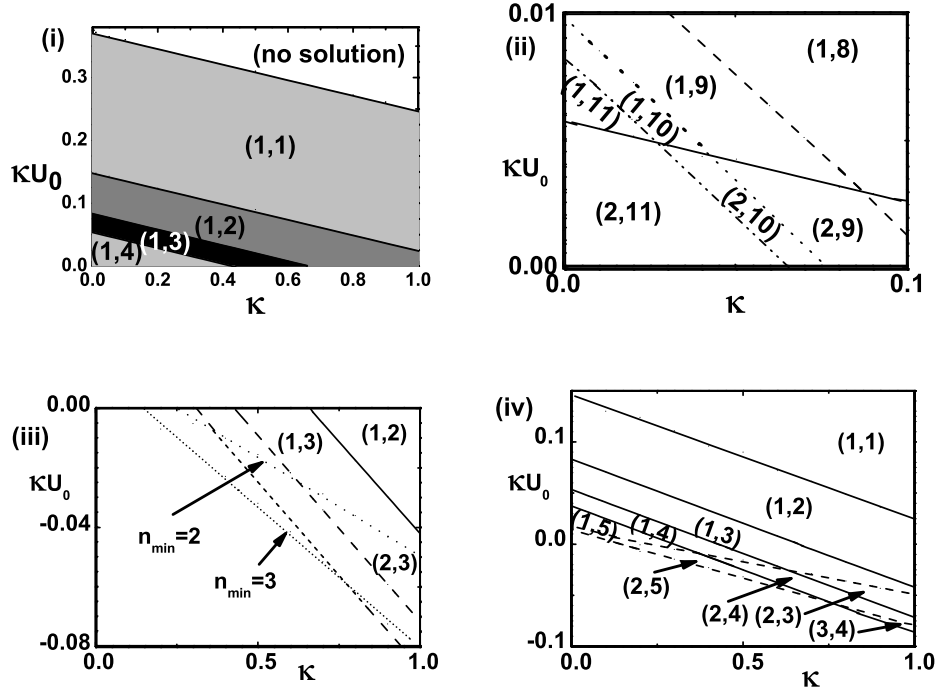


Figure 9: Oscillating behaviors depending on  $\tilde{\kappa}$  and  $\tilde{\kappa}\tilde{U}_o$ . Figure(i) shows oscillating properties of dS-dS degenerate case and figure(ii) shows small value of parameters once more. Figure(iii) is a AdS-AdS degenerate case, and figure(iv) shows total parameter space, we have searched.

region corresponding to regions in which  $\tilde{U}_o \leq -0.125$  in the case of AdS-AdS degenerate vacua because there is no dS region of potential [7]. In this case, the change of  $n_{min}$  is more remarkable. Even at the  $\tilde{\kappa} = 1$ , it means very strong gravity, the change of  $n_{min}$  occurs. This point is another difference between the dS-dS and the AdS-AdS. Whole parameter space of  $\tilde{\kappa}$  and  $\tilde{\kappa}\tilde{U}_o$  is shown in fig. (iv). In this figure, we can see the changes of  $n_{min}$  and  $n_{max}$  in the dS-dS are continuously connected to those in the AdS-AdS. The  $x$ -axis,  $\tilde{U}_o = 0$ , represents the flat-flat case. In the flat-flat case, there exists a solution for all of  $\tilde{\kappa}$  except when  $\tilde{\kappa} = 0$ .

Figure 10 shows the schematic diagram of the phase space of all solutions including another type solution and the number of oscillating solutions with different  $\tilde{\kappa}$ s. The left figure has  $\tilde{\kappa} = 0$  line indicating no gravity effect. There is the zone representing no solution in the right upper region in the case of the dS. The dS region has positive  $\tilde{U}_o$  and the AdS region has negative  $\tilde{U}_o$  divided by the line,  $\tilde{U}_o = 0$ , representing the flat case. In the middle area including the flat case,  $n_{min}$  and  $n_{max}$  increase as  $\tilde{\kappa}$  and  $\tilde{\kappa}\tilde{U}_o$  decrease. The tendencies are indicated as the arrows. The inclined line in AdS region represents  $\tilde{U}_o = -0.125$  or  $\tilde{U}_{top} = 0$ . In the left lower region, there exist another type solution. The right figure shows  $n_{min}$  and  $n_{max}$  are changed in terms of  $\tilde{\kappa}\tilde{U}_o$  and  $\tilde{\kappa}$ . As we can see from the figure,  $n_{max}$  and  $n_{min}$  increase as  $\tilde{\kappa}\tilde{U}_o$  decreases.

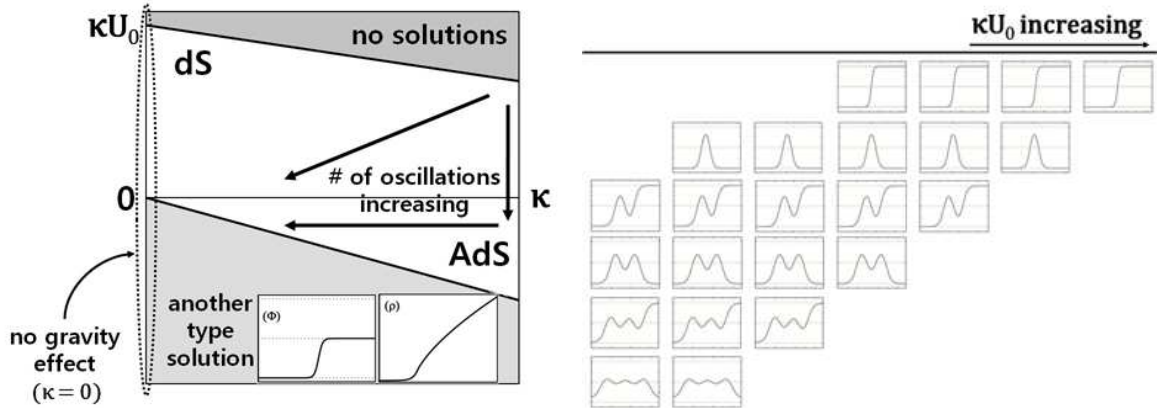


Figure 10: Illustrations of the phase space of solutions and oscillating properties. Left figure shows a whole solution space, and right figure shows number of oscillating solutions changing on given  $\kappa$ .

Figure 11 shows another type solutions in Fig. 10. The solutions represent the tunneling from the top of the potential, a point of an unstable equilibrium, to the local vacuum state instead of rolling down the potential. The solutions can be a kind of the bubble solution describing tunneling without a barrier [31, 32]. In the figures (i)s, we take  $\tilde{\kappa} = 0.5$  and  $\tilde{U}_o = -0.125$ . The inside geometry is AdS and outside flat. In the figures (ii)s, we take  $\tilde{\kappa} = 0.5$  and  $\tilde{U}_o = -1$ . The inside geometry is AdS and outside AdS.

## 5 Summary and Discussions

We have studied oscillating instanton solutions of a self-gravitating scalar field between degenerate vacua. We obtained numerical solutions not only in dS but also in both flat and AdS space. Furthermore, we constructed the phase space of all our solutions including the number of oscillations. As a by-product, we obtained the solution describing tunneling without a barrier. Basically, our method for obtaining the domain wall or braneworld-like object [33, 34] is based on the instanton-induced theory rather than the kink-induced theory. Our approach is related to the question: How we can make spacetime including the domain wall even in flat or AdS space? If the thin-wall approximation scheme is allowed in our work and the mechanism is applied to solutions in higher-dimensional theories, our one-crossing solutions can be interpreted as the mechanism providing nucleation of the domain wall or braneworld in instanton-induced theory. Because our oscillating solutions have a thick wall with varying energy density, our oscillating solutions can be interpreted as the mechanism providing nucleation of the thick wall for topological inflation [35, 36].

In Sec. II, we analyzed the boundary conditions of our problem. There are two kinds of conditions. We imposed the boundary conditions as the initial value problem and imposed additional conditions implicitly. We obtained the initial value  $\tilde{\Phi}_o$  by employing the undershoot-

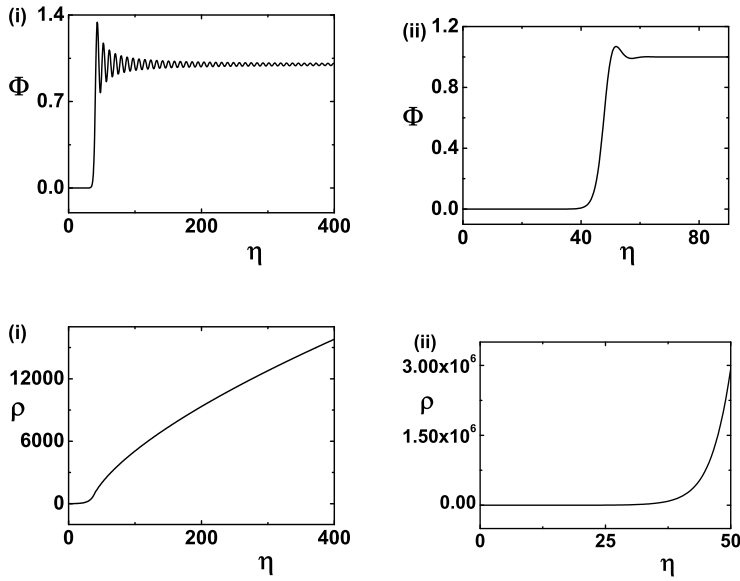


Figure 11: The solutions describing tunneling without a barrier. The upper two figures show the solution of  $\tilde{\Phi}$  and the lower two figures show the solution of  $\tilde{\rho}$ .

overshoot procedure. To avoid a singular solution at  $\tilde{\eta} \rightarrow \tilde{\eta}_{max}$  in Eq. (10) and demand the  $Z_2$  symmetry, the conditions  $d\tilde{\Phi}/d\tilde{\eta} \rightarrow 0$  and  $\tilde{\rho} \rightarrow 0$  as  $\tilde{\eta} \rightarrow \tilde{\eta}_{max}$  were needed.

In Sec. III, we obtained the numerical solution of oscillating instantons. In particular, we performed the numerical work with more detail for the cases in flat space, and in both dS and AdS space. The number of oscillations increases as the initial point,  $\tilde{\Phi}(\tilde{\eta}_{initial}) = \tilde{\Phi}_0$ , moves away from the vacuum state. We can see that the size of the geometry of solutions decreases as the number of crossing increases because the period of the evolution parameter  $\tilde{\eta}_{max}$  decreases as the starting point moves away from the vacuum state. As expected, this type of solutions is possible only if gravity is taken into account. The maximum number of oscillations is determined by the parameters  $\tilde{\kappa}$  and  $\tilde{U}_0$  observed in Ref. [23]. The solutions are of two types. One type is for situations in which different parts of spacetime are in different vacua. The solutions representing tunneling which go from the left vacuum state to the right vacuum state have a non-zero topological charge. The other type is for situations in which different parts of spacetime are in the same vacuum state. Others representing the solutions which go back to the starting point after oscillations have zero topological charge. We can see that the sign change of  $\tilde{\rho}'$  from positive to negative occurs at the half period of  $\tilde{\eta}$  due to the  $Z_2$  symmetry. We have studied the behavior of the solutions in the  $\tilde{\Phi}(\tilde{\eta})$  -  $\tilde{\Phi}'(\tilde{\eta})$  plane using the phase diagram method. Figures (i), (iii), and (v) have symmetry about the  $y$ -axis, while figures (ii), (iv), and (vi) have symmetry about the  $x$ -axis. The maximum value of  $\tilde{\Phi}'$  decreases as the number of crossing increases. We have checked the energy density diagrams for each

solutions. The peaks of the volume energy density broaden in range near  $U_{top}$  as the number of crossing increases. The shape of peaks of the surface energy density becomes smooth and broadens as the number of crossing increases. We have examined which solutions among the oscillating solutions are relatively probable. Instead of subtracting the background action from the instanton action, we compared the action of oscillating solutions with the action of the one-crossing instanton. Our results show that, as predicted, the transition amplitude is suppressed by an increase in oscillation number.

In Sec. IV, we obtained the phase space of solutions in terms of the parameters  $\tilde{\kappa}$  and  $\tilde{\kappa}\tilde{U}_o$ . To make the phase space of solutions, we collected data on  $\tilde{U}_o$ , which makes the difference of the maximum number of oscillations,  $n_{max}$ , for a given  $\tilde{\kappa}$ . We then obtained a specific  $\tilde{U}_o$  which determines the minimum number of oscillations,  $n_{min}$ . Finally, we employed the method of least squares [28] to obtain the relationship between two parameters in given data sets of  $\tilde{\kappa}$  and  $\tilde{\kappa}\tilde{U}_o$ . Oscillating numbers appeared to be linearly related to the parameters. Figure 9 shows the behaviors of oscillating solutions in terms of  $\tilde{\kappa}$  and  $\tilde{\kappa}\tilde{U}_o$ . The value of  $\tilde{\kappa}$  is limited to  $0 \leq \tilde{\kappa} \leq 1$ . At the point  $\tilde{\kappa} = 0$ , or  $M_p = \infty$ , gravity is switched off. The  $y$ -axis represents no gravity. We expect that there is no solution with  $O(4)$  symmetry when gravity is switched off. When the parameter  $\tilde{\kappa}$  or  $\tilde{U}_o$  increased, the evolution period of  $\tilde{\eta}_{max}$  diminished in general. When the parameter  $\tilde{\kappa}$  or  $\tilde{U}_o$  decreased, the evolution period of  $\tilde{\eta}_{max}$  and the maximum number of oscillations increased. There is a no-solution parameter region corresponding to regions in which  $\tilde{U}_o \leq -0.125$  in the case of AdS-AdS degenerate vacua because there is no dS region of potential [7]. We can see the changes of  $n_{min}$  and  $n_{max}$  in the dS-dS are continuously connected to those in the AdS-AdS. The  $x$ -axis,  $\tilde{U}_o = 0$ , represents the flat-flat case. In the flat-flat case, there exists a solution for all of  $\tilde{\kappa}$  except when  $\tilde{\kappa} = 0$ . Figure 10 shows the schematic diagram of the phase space of all solutions including another type solution and the number of oscillating solutions with different  $\tilde{\kappa}$ s.

As a result of this tunneling, a finite-sized geometry with  $Z_2$  symmetry is obtained. Our mechanism for making the domain wall or braneworld-like object is different from the ordinary formation mechanism of the domain wall because our solutions are instanton solutions rather than soliton solutions. In other words, our solutions can be interpreted as solutions describing an instanton-induced domain wall rather than a kink-induced domain wall or braneworld-like object. Domain walls can form in any model having a spontaneously broken discrete symmetry. An inertial observer sees the domain wall accelerating away with a specific acceleration. The domain wall has repulsive gravitational fields [37, 38]. The thickness of the domain wall in flat spacetime can be estimated by a balance between the potential energy and the gradient energy. When the thickness of the domain wall is greater than or equal to the horizon size corresponding to the vacuum energy in the interior of the domain wall, topological inflation can occur. The scalar field stays near the top of the potential at the core. This potential energy serves as a vacuum energy in a similar way to the slow-rollover inflationary models. This topological inflation does not require fine-tuning of the initial conditions and is eternal even at the classical level due to the topological reason. Our oscillating instanton solutions can be interpreted as mechanism providing the nucleation of the thick wall for the topological inflation, even though

we started in flat or AdS space. The wrinkles representing the variation of the volume energy density in the wall may be interpreted as density perturbations in the inflating region. In this work, inflating regions described by the oscillating solutions and density perturbations described by the variation of energy density can occur simultaneously. Furthermore, oscillating bounce solutions also have the thick wall. Thus we expect that (non-)topological inflation can be made by oscillating bounce solutions.

To obtain the dynamics of the solutions, we should apply the analytic continuation from Euclidean to Lorentzian signature. If the wall is thin, we can employ the Israel junction condition [7, 39] or the method [10, 40]. If the wall is thick, the double-null simulation may be more relevant to the dynamics of the solutions [41].

Future research could whether or not our solutions obtained using instanton-induced theory can be extended to theories with gauge fields or various dimensions and whether or not the topological charge of both instantons and bounce solutions, including oscillating solutions, can be well-defined and conserved for a self-gravitating scalar field in various dimensions. It would also be interesting to examine if this toy model with the variation of energy density can provide a proper inflationary scenario. In Ref. [42], the creation of a charged black hole pair separated by a thin domain wall and the dynamics of the domain wall were studied in the cosmological context. It would be interesting to study the properties and evolution of topological inflation with a magnetic field.

## 6 Acknowledgements

We would like to thank E. J. Weinberg, Yun Soo Myung, Soonkeon Nam, Hongsu Kim, Jungjai Lee, Gungwon Kang, Youngone Lee, Hyeong-Chan Kim, Hyun Seok Yang, In Yong Park, and Dong-han Yeom for helpful discussions and comments. This work was supported by the Korea Science and Engineering Foundation (KOSEF) grant funded by the Korea government(MEST) through the Center for Quantum Spacetime(CQuST) of Sogang University with grant number R11 - 2005 - 021. WL was supported by the National Research Foundation of Korea Grant funded by the Korean Government (Ministry of Education, Science and Technology)[NRF-2010-355-C00017].

## References

- [1] A. Belavin, A. Polyakov, A. Schwartz, and Y. Tyupkin, Phys. Lett. **59B**, 85 (1975); G. 'tHooft, Phys. Rev. D **14**, 3432 (1976); Phys. Rev. Lett. **37**, 8 (1976); C. G. Callen, Jr., R. Dashen, and D. Gross, Phys. Lett. **63B**, 334 (1976).
- [2] S. Bolognesi and K. Lee, arXiv:1106.3664.
- [3] G. Gibbons, M. Green, and M. Perry, Phys. Lett. B **370**, 37 (1996); A. V. Belitsky, S. Vandoren, and P. van Nieuwenhuizen, Classical Quantum Gravity **17**, 3521 (2000).
- [4] S. Vandoren and P. van Nieuwenhuizen, arXiv:0802.1862.
- [5] S. W. Hawking, Phys. Lett. **60A**, 81 (1977); G. W. Gibbons and S. W. Hawking, Phys. Lett. **78B**, 430 (1978); T. Eguchi, P. B. Gilkey and A. J. Hanson, Phys. Rept. **66**, 213 (1980); G. 'tHooft, Nucl. Phys. **B315**, 517 (1989); H. Kim and Y. Yoon, Phys. Rev. D **63**, 125002 (2001); D. N. Page, arXiv:0912.4922; J. J. Oh, C. Park, and H. S. Yang, J. High Energy Phys. 04 (2011) 087.
- [6] S. Coleman, *Aspects of symmetry* (Cambridge University Press, 1985).
- [7] B.-H. Lee, C. H. Lee, W. Lee, and C. Oh, Phys. Rev. D **82**, 024019 (2010).
- [8] M. B. Voloshin, I. Yu. Kobzarev, and L. B. Okun, Yad. Fiz. **20**, 1229 (1974) [Sov. J. Nucl. Phys. **20**, 644 (1975)].
- [9] S. Coleman, Phys. Rev. D **15**, 2929 (1977); *ibid.* D **16**, 1248(E) (1977).
- [10] S. Coleman and F. De Luccia, Phys. Rev. D **21**, 3305 (1980).
- [11] S. Parke, Phys. Lett. **121B**, 313 (1983).
- [12] S. W. Hawking and I. G. Moss, Phys. Lett. **110B**, 35 (1982).
- [13] L. G. Jensen and P. H. Steinhardt, Nucl. Phys. **B237**, 176 (1984); **B317**, 693 (1989); J. Garriga and A. Vilenkin, Phys. Rev. D **57**, 2230 (1998); T. Banks, arXiv:hep-th/0211160; E. J. Weinberg, Phys. Rev. Lett. **98**, 251303 (2007); S.-H. Henry Tye, D. Wohns, and Y. Zhang, Int. J. Mod. Phys. A **25**, 1019 (2010).
- [14] T. Banks and M. Johnson, hep-th/0512141; A. Aguirre, T. Banks, and M. Johnson, J. High Energy Phys. 08 (2006) 065; R. Bousso, B. Freivogel, and M. Lippert, Phys. Rev. D **74**, 046008 (2006).
- [15] B. Kumar, M. B. Paranjape, and U. A. Yajnik, Phys. Rev. D **82**, 025022 (2010).
- [16] J. J. Blanco-Pillado, D. Schwartz-Perlov, and A. Vilenkin, J. Cosmol. Astropart. Phys. 12 (2009) 006; J. Cosmol. Astropart. Phys. 05 (2010) 005.

- [17] K. Lee and E. J. Weinberg, Phys. Rev. D **36**, 1088 (1987).
- [18] Y. Kim, K. Maeda, and N. Sakai, Nucl. Phys. **B481**, 453 (1996); Y. Kim, S. J. Lee, K. Maeda, and N. Sakai, Phys. Lett. B **452**, 214 (1999).
- [19] W. Lee, B.-H. Lee, C. H. Lee, and C. Park, Phys. Rev. D **74**, 123520 (2006).
- [20] R.-G. Cai, B. Hu, and S. Koh, Phys. Lett. B **671**, 181 (2009).
- [21] H. Kim, B.-H. Lee, W. Lee, Y. J. Lee, and D.-h. Yeom, arXiv:1011.5981; B.-H. Lee, W. Lee, and D.-h. Yeom, J. Cosmol. Astropart. Phys. 01 (2011) 005.
- [22] B.-H. Lee and W. Lee, Classical Quantum Gravity **26**, 225002 (2009).
- [23] J. C. Hackworth and E. J. Weinberg, Phys. Rev. D **71**, 044014 (2005); E. J. Weinberg, AIP Conf. Proc. **805**, 259 (2006).
- [24] C. G. Callan, Jr. and S. Coleman, Phys. Rev. D **16**, 1762 (1977); E. J. Weinberg, Phys. Rev. D **47**, 4614 (1993); J. Baacke and V. G. Kiselev, Phys. Rev. D **48**, 5648 (1993); A. Strumia and N. Tetradis, J. High Energy Phys. 11 (1999) 023; J. Baacke and G. Lavrelashvili, Phys. Rev. D **69**, 025009 (2004); G. V. Dunne and H. Min, Phys. Rev. D **72**, 125004 (2005); H. Min, J. Phys. A: Math. Gen. **39**, 6551 (2006); D. Metaxas, Phys. Rev. D **75**, 065023 (2007).
- [25] T. Tanaka and M. Sasaki, Prog. of Theor. Phys. **88**, 503 (1992); T. Tanaka, Nucl. Phys. **B556**, 373 (1999); A. Khvedelidze, G. Lavrelashvili, and T. Tanaka, Phys. Rev. D **62**, 083501 (2000); G. Lavrelashvili, Nucl. Phys. Proc. Suppl. **88**, 75 (2000); Phys. Rev. D **73**, 083513 (2006); G. V. Dunne and Q.-h. Wang, Phys. Rev. D **74**, 024018 (2006).
- [26] J. W. York, Jr., Phys. Rev. Lett, **28**, 1082 (1972); G. W. Gibbons and S. W. Hawking, Phys. Rev. D **15**, 2752 (1977); J. W. York, Jr., Found. Phys. **16**, 249 (1986).
- [27] B. K. Berger, Gen. Rel. Grav. **38**, 625 (2006).
- [28] W. H. Press, S. A. Teukolsky, W. T. Vetterling, and B. P. Flannery, *Numerical Recipes in Fortran* (Cambridge, 1992).
- [29] G. W. Gibbons, S. W. Hawking, and M. J. Perry, Nucl. Phys. **B138**, 141 (1978).
- [30] R. Bousso and A. Linde, Phys. Rev. D **58**, 083503 (1998).
- [31] K. Lee and E. J. Weinberg, Nucl. Phys. **B246**, 354 (1986); K. Lee, Nucl. Phys. **B282**, 509 (1987).
- [32] L. G. Jensen and P. H. Steinhardt, Nucl. Phys. **B317**, 693 (1989).

- [33] L. Randall and R. Sundrum, Phys. Rev. Lett. **83**, 3370 (1999); Phys. Rev. Lett. **83**, 4690 (1999).
- [34] P. D. Mannheim, *Brane-Localized Gravity* (World Scientific, 2005).
- [35] A. Vilenkin, Phys. Rev. Lett. **72**, 3137 (1994); A. Linde, Phys. Lett. B **327**, 208 (1994).
- [36] N. Sakai, H. Shinkai, T. Tachizawa, and K. Maeda, Phys. Rev. D **53**, 655 (1996); I. Cho and A. Vilenkin, Phys. Rev. D **56**, 7621 (1997).
- [37] A. Vilenkin, Phys. Lett. **133B**, 177 (1983).
- [38] J. Ipser and P. Sikivie, Phys. Rev. D **30**, 712 (1984).
- [39] W. Israel, Nuovo Cimento B **44**, 1, (1966); *ibid.* B **48**, 463(E) (1967).
- [40] C. H. Lee and W. Lee, J. Korean Phys. Soc. **45**, S1 (2004).
- [41] D.-i. Hwang and D.-h. Yeom, arXiv:1010.3834; J. Hansen, D.-i. Hwang, and D.-h. Yeom, J. High Energy Phys. 11 (2009) 016; S.-E. Hong, D.-i. Hwang, E. D. Stewart, and D.-h. Yeom, Classical Quantum Gravity **27**, 045014 (2010).
- [42] B. Gwak, B.-H. Lee, W. Lee, and M. Minamitsuji, arXiv:1101.5748; S. H. Mazharimousavi and M. Halilsoy, Phys. Lett. B **697**, 497 (2011); B.-H. Lee, W. Lee, and M. Minamitsuji, Phys. Lett. B **679**, 160 (2009).